Journal of Dynamics, Monitoring and Diagnostics, 2024, 3, 40-48
https://doi.org/10.37965/jdmd.2024.501

ISTP
RESEARCH ARTICLE

Exploring the Limits of a Deflection-Based Method for the Estimation of Dynamic Stress in Beams

Archie Keys and Jordan Cheer
Institute of Sound and Vibration Research, University of Southampton, Southampton, SO17 1BJ, UK

(Received 22 December 2023; Revised 21 February 2024; Accepted 01 March 2024; Published online 06 March 2024)

Abstract: Estimation of the dynamic stress in structures, such as beams and plates, has previously been made using the relationship between stress and velocity spatial maxima based on far-field assumptions. This paper presents a method for the estimation of dynamic stress in a beam using Euler–Bernoulli beam theory, where deflection data from a grid of measurement points on the surface of the beam is used to estimate the dynamic bending stress in the structure. The limitations of the method are investigated via response data provided by a numerical model of a free-free beam. A nondimensional wavenumber analysis is used to determine the number of points required for an accurate estimate of stress. Beams with a range of material and geometric parameters are modeled in order to explore the limits of the estimation method, and parameters representative of several real-world materials are used to assess the suitability of the method for practical applications.

Keywords: Beams; dynamic stress; structural dynamics; vibration

I. INTRODUCTION

Traditional methods for the measurement of stress in a structure make use of strain gauges, along with knowledge of the Young's modulus of the material, to directly obtain stress at a given point. This method, however, faces several potential limitations. First, the application of strain gauges to lightweight structures will modify the effective mass and stiffness of the structure and thus impact its dynamic behavior. While this effect may be negligible in many situations, it can become significant when the structure is lightweight. The increasing drive to use lightweight structures in many engineering applications means that this effect more frequently limits the use of a strain gauge-based measurement approach. Another limitation of strain gauge-based measurements is that the strain is measured over a distributed area of the structure, such that highly localized stress concentrations cannot be resolved.

One approach to overcome the limitations of stress characterization is to utilize a laser doppler vibrometer, which as a noncontact method does not influence the dynamics of the structure and offers the potential for high-resolution characterization of the structure via measurements over a fine grid of points. However, this approach is indirect, requiring the dynamic stress to be estimated from the measured velocity response.

The relationship between structural velocity and dynamic stress was initially investigated by Hunt [1] and Ungar [2], who explored the ratio of dynamic stress to velocity for a range of beams and plates vibrating at resonance. This work was subsequently applied to pipes vibrating at their first modal frequency by Wachel [3], who made estimates of the maximum dynamic stress in a structure from measurements of the overall maximum velocity. Following this, Fahy [4,5] and Stearn [6,7] analytically predicted the spatial variation of stress, strain, and acceleration in large plates and cylinders subject to multimodal excitation. This analysis assumes a multimode diffuse bending wave field, where many vibrational modes are excited by a broadband excitation. This allows simplifications to be made to the relationship between transverse vibrational velocity and stress in the structure, since for a multimode diffuse bending wave field the mean-square vibrational velocities are independent of angular position, and the waves in the structure are assumed to be statistically independent from each other. This relationship was experimentally validated by Norton and Fahy [8], who estimated the dynamic stress in fluid-filled pipes using measurements of acceleration. These estimates were validated against measurements taken directly from the same point on the structure using strain gauges. A narrow band excitation method for the estimation of dynamic stress was proposed by Karczub [9,10], in which a prediction of the maximum overall dynamic stress was obtained by predicting the spatial maximum stress in each frequency band and then summing the values. This method makes a far-field assumption, so it is only valid away from sources of evanescent waves in the structure and was implemented experimentally for beams, plates, and shells [9,10]. The use of finite difference formulations to estimate the dynamic stress in a structure was also explored by Karczub [11], where measurements of velocity at three points on a beam were taken to estimate the stress at the central point using Euler–Bernoulli beam theory. This method does not make a far-field assumption, so it can be implemented at any point where there is space to apply three sensors.

The related inverse problem of estimating displacement, velocity, or acceleration from measurements of strain has also been considered by both Hong [12] and Park [13] for a beam. Park [13] used Euler–Bernoulli beam theory to relate the second spatial derivative of beam deflection to dynamic strain in a structure, which allows beam deflection to be estimated using strain gauge data via a double integration. Hong [12] uses an alternative method to achieve the same results, implementing a moment-area method to estimate beam deflection from strain responses. The spatial distribution of stress on a micro-cantilever beam

Corresponding author: A. Keys (e-mail: a.keys@soton.ac.uk).

was estimated by Tamayo [14], who used an optical microscopy method to measure dynamic beam deflection across the surface of the structure, before implementing Euler–Bernoulli beam theory to calculate the dynamic stress based on the identified mode shapes. This method was tested for both experimentally and numerically obtained responses and showed only small differences in the mode shapes and their frequencies. However, the method was only implemented at the modal frequencies of the system, since the input force was made up of several frequency components, each relating to one of the predicted modal frequencies from the numerical study.

This work presents a method for the estimation of dynamic bending stress in a uniform beam using Euler–Bernoulli beam theory. The estimation is implemented using deflection data obtained from a grid of points across the surface of the structure and allows the stress to be estimated at any of these points over a broad frequency range. There are two main potential advantages to this method compared to the velocity spatial maxima methods described above [4–7]: it can be applied to the entire geometry of the structure, not just in the far-field, and it does not assume a diffuse field, allowing it to be implemented at individual frequencies. Some of the methods that relate stress to velocity spatial maxima are not limited by the type of excitation [9,10], so the method presented in this paper only has the advantage of being applicable in the presence of evanescent waves. Additionally, compared to [11], where Euler–Bernoulli beam theory is applied to the calculation of stress at a single point on a structure, the investigated method uses a large grid of points distributed across the structure to allow the spatial variation of the stress to be estimated.

Miles and Xu [15,16] have previously utilized the same method explored in this paper to experimentally measure the dynamic strain power spectral density (PSD) in both beams and plates for a random excitation. Moccio [17] has also applied the method to calculate the transfer function between input force and dynamic strain for a cantilever beam, applying polynomial functions to smooth the spatial experimental data in order to increase the accuracy of the estimation. This paper presents an application of the same method to a free-free beam to estimate the dynamic stress and explores the limitations of the method when applied to beams with a range of geometrical and material parameters.

The paper is structured as follows: Section II outlines the method used to estimate stress using Euler–Bernoulli beam theory, before Section III describes the numerical model that is used to investigate the method. Section IV presents an investigation of the stress estimation method, discussing how the number of points influences the accuracy of the estimation, how the consistency of the method varies across the geometry of the beam, and its ability to estimate stress response shapes. Section V presents a parametric study of how the material and geometric properties of the beam influence the limits of the stress estimation method. Section VI applies the estimation procedure to beams constructed from commonly utilized materials, and Section VII draws conclusions based on the work.

II. STRESS ESTIMATION METHOD

In this section, the method used to estimate stress based on deflection data at discrete points on a beam is outlined, detailing how Euler–Bernoulli beam theory can be used to calculate bending stress from the second spatial derivative of beam deflection.

Euler–Bernoulli beam theory gives a simple analytical relationship between the bending stress in a beam, σ, and the second spatial derivative of beam deflection, w, as [18:]

$$\sigma = -zE\frac{d^2w}{dx^2}, \tag{1}$$

where z is the distance between the neutral axis of the structure and the point at which stress is being calculated and E is the Young's modulus of the material from which the beam is constructed. In this work, the value for z is taken as half of the thickness of the uniform beam, meaning that the stress calculated using Equation 1 will be an estimate of the stress on the surface of the beam and will represent the maximum value of stress for each position in x and y.

In order to evaluate the second spatial derivative of beam deflection, a uniformly spaced grid of points across the surface of the beam is implemented, as shown in Fig. 1. The gradient of beam deflection is calculated separately for each of the rows of points along the length of the beam, since only bending stress in the x direction is under consideration in this work. In order to numerically calculate the gradient along each of the three rows of points, a function is implemented which uses a central difference calculation for interior points and a single-sided difference calculation for points on the edge of each of the three deflection vectors. It is important to note that this may decrease the accuracy of the stress estimation at the points at either end of the beam. This gradient function is used to calculate d^2w/dx^2, allowing stress to be estimated at each of the grid of points by evaluating Equation 1.

A. GRADIENT CALCULATION ERROR

The numerical gradient function used to calculate d^2w/dx^2 will introduce some degree of error into the stress estimation method. It is useful to quantify this error so that when analyzing the estimated stress, it is understood whether errors are due to the gradient calculation or other factors.

In order to assess the error, an analytical function has been assumed as:

$$f(x) = A\,cos(\omega x), \tag{2}$$

where ω and A are parameters controlling the frequency and amplitude of the function, respectively. This function has been chosen because its derivative is simple to calculate analytically, giving an accurate basis for an error estimate,

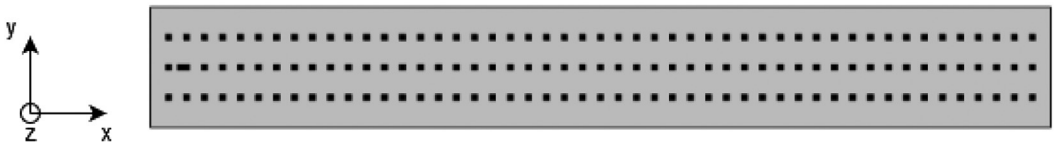

Fig. 1. Numerical model geometry showing the grid of points from which deflection data is used to estimate stress.

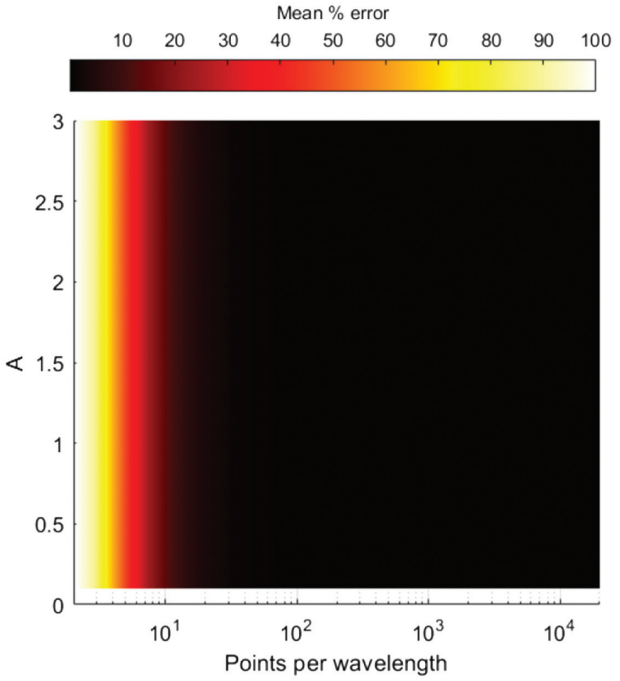

Fig. 2. Mean percentage error in the gradient calculation for a range of values of A and points per wavelength.

and it represents a possible analytical mode shape of the structure. In order to assess the error in the numerical estimation of the gradient, the second derivative of $f(x)$ has been calculated both analytically and using the gradient function. In both cases, the function is sampled at evenly spaced points in x, and the percentage error is calculated at each point. The overall error in the estimation is then quantified by taking an average of the percentage error over the positions in x. Figure 2 shows the mean percentage error for a range of values of both A and the number of points per wavelength used in the estimation. Inspection of this plot shows that the amplitude of $f(x)$ does not influence the error; however, the error significantly varies with the number of evaluation points per wavelength. Specifically, low error is observed when the number of points per wavelength is high but increases as the number of points decreases such that the error is approximately 10% at around 10 points per wavelength. This demonstrates that the error associated with the numerical gradient function is not significant, provided that a sufficiently large number of points are utilized in the stress estimation.

III. NUMERICAL MODEL

This section describes the numerical model used to investigate the method of estimating stress in a beam outlined in Section II and defines the parameters used to describe the model.

Table I. Parameter values used to define the numerical model

Parameter	Symbol	Value
Beam thickness	h	5 mm
Beam length	l	300 mm
Beam width	b	40 mm
Points in x direction	K	49
Points in y direction	L	3
Force x coordinate	F_x	10 mm
Excitation force	F	1 N
Young's modulus	E	70 GPa
Density	ρ	2728 kg/m^3
Isotropic loss factor	η	0.2

A 2D numerical model of a uniform beam has been implemented using COMSOL Multiphysics software using finite elements. The nominal parameters used to describe the model geometry are defined in Fig. 3, with their values listed in Table I along with the assumed material parameters. These parameter values have been chosen to approximate aluminum alloy 8082-T6 with an applied viscoelastic damping layer and should be assumed in the following sections unless stated otherwise.

The numerical model assumes that the beam is constructed from a linear elastic material which is given a stiffness of E and a density of ρ, while the material damping is modeled using an isotropic loss factor, η. A force is applied near to one end of the beam, positioned centrally in the y direction and at a distance of F_x from the end of the beam. The force acts in the z direction with magnitude F, and the boundary conditions along all edges of the beam are free. A K by L grid of points is defined on the surface of the beam, with equal spacing in both x and y directions, allowing beam deflection data to be extracted and used to estimate the stress. The model is solved between 100 Hz and 3 kHz with a frequency spacing of 10 Hz.

IV. VALIDATION OF THE ESTIMATION METHOD

This section presents a validation of the stress estimation method described in Section II when applied to the data obtained from the numerical model of a uniform beam described in Section III. Initially, the effect of varying the number of points utilized in the stress estimation procedure is explored. Subsequently, both the estimation error and the stress amplitude are investigated for a range of positions on the beam.

Fig. 3. Numerical model geometry showing definitions for the beam length, width, and thickness parameters.

A. NUMBER OF POINTS

In order to obtain an accurate estimation of the stress in a beam, the second spatial derivative of beam deflection must be accurately obtained. This requires deflection data to be taken at a sufficient number of points along the length of the beam. The resolution of this spatial sampling must be chosen such that the number of points per wavelength at the highest frequency of interest is sufficient to resolve the shape of the beam deflection. In Section V, a wide range of material parameters will be explored, including those that result in a very small wavelength of vibration in the beam. It is important, therefore, that the number of points required for an accurate estimation of stress for a given set of material and geometric parameters is assessed. In order to carry out this assessment, values of E and ρ that sit at the center of the range of values under consideration in Section V have been chosen, allowing the minimum number of points required for an accurate estimation to be determined.

To explore the effect of varying the grid resolution, the stress estimation procedure has been carried out for values of K equal to 9,19,29,49,69, and 99; these values have been chosen because they all result in a point at the center of the beam in the x direction and thus allow a straightforward means of comparing estimation accuracy at this consistent point. Figure 4 shows the stress directly exported from the numerical model, along with the stress estimated using the method outlined in Section II at the center point of the beam for the different grid resolutions. Examination of Fig. 4 shows that increasing the number of points used to carry out the stress estimation increases its accuracy, and that the estimation accuracy tends to decrease with increasing frequency. This is expected, since both an increase in frequency and a decrease in the number of points used result in a reduction in the number of points per wavelength.

To quantify this effect, a nondimensional wavenumber, ν, is defined as:

$$\nu = \frac{\Delta}{\lambda}, \tag{3}$$

where Δ is the spacing between two adjacent points along the length of the beam, given by $l/(K+1)$, and λ is the wavelength of vibration. For a uniform beam, this can be calculated from material and geometric parameters as:

$$\lambda = \left(\frac{Eh^2}{12\rho}\right)^{\frac{1}{4}} 2\pi\omega^{-\frac{1}{2}}, \tag{4}$$

where ω is the angular frequency of vibration. It is typical to require approximately 10 points per wavelength in order to properly resolve the shape of a wave [19], which in this case corresponds to a wavenumber of $\nu = 0.1$. The frequency at which this wavenumber occurs is marked on Fig. 4 with a star for each of the cases under consideration, showing the frequency above which $\nu > 0.1$. Inspection of Fig. 4 shows that the frequency range for which $\nu < 0.1$ increases with the number of points used, and that using 69 or 99 points in this case results in the $\nu = 0.1$ point occurring above the highest frequency considered.

To quantify the error between the estimated and directly evaluated stress, the mean percentage error across frequency is shown in Table II for each number of points used. The values in Table II show that the mean percentage error decreases as the number of points used increases up to the 49-point configuration, after which the error actually increases slightly, but at a much slower rate. This is caused by small numerical rounding errors which are amplified when the second derivative is taken, resulting in a slight overestimate of the stress. This effect is more significant when there are more points per wavelength because the difference between the points becomes less and, therefore, the small numerical rounding error becomes relatively more significant.

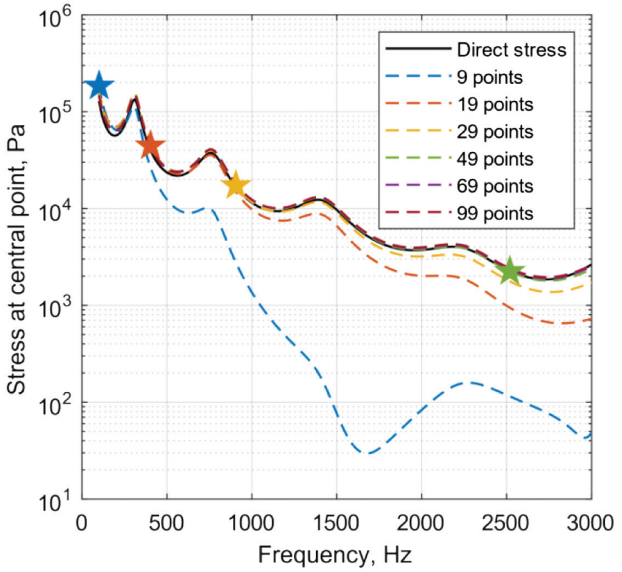

Fig. 4. Stress against frequency at the center point along the length of the beam for different numbers of points, with the frequency at which $\nu = 0.1$ occurs marked for each case.

Based on the results presented in this section, the 49-point configuration is best suited to the considered structure, since the frequency at which $\nu = 0.1$ is close to the highest frequency of interest, and the mean percentage error is the lowest for the values of K considered. Going forward, parameter values will be explored that result in considerably shorter wavelengths than for the beam case considered here; however, based on these results, the number of points used should be chosen such that $\nu < 0.1$ for the entire frequency range of interest for all parameter values. In the remainder of this section, the parameter values listed in Table I will be used, including the number of points along the length of the beam, $K = 49$, since this results in more than 10 points per wavelength over the frequency range of interest for these parameters.

Table II. Mean percentage error at the central point on the beam for the numbers of points K

K	Mean % error
9	82
19	34
29	14
49	5.8
69	6.4
99	7.2

B. POSITION ON THE BEAM

The previous section considered the accuracy of the estimation at a single point on the beam; however, it is important to consider the accuracy of the estimation procedure across the structure.

One of the assumptions made in the Euler–Bernoulli beam theory on which the estimation method is based is that the stress does not vary significantly over the width of the beam. This assumption is expected to be valid provided that the wavelength of vibration is significantly greater than the width of the beam. To validate this assumption, the stress directly evaluated in the numerical model is compared to the estimated stress at three points across the width of the beam at a point halfway along the length and the results are presented in Fig. 5. These results show that there is no significant variation in the stress across the width of the beam for either the directly exported or the estimated stress for the beam parameters defined in Table I.

It is also important to investigate how the estimation accuracy varies along the length of the beam. The stress estimation has been carried out at all 49 positions along the length of the beam, at the center position across the width. To quantify the error in a way that shows changes in the error at low levels, an error is defined as:

$$error = 20\log_{10}\left|\frac{\sigma_e - \sigma_d}{\sigma_d}\right| \text{dB} \tag{5}$$

where σ_e is the estimated stress and σ_d is the direct stress. This error is shown for the frequency range of interest at each of the considered points in Fig. 6. These results show a low percentage error, approximately −20 to −40 dB, for the majority of the beam across all frequencies, with the error in the estimation decreasing as frequency increases. This is due to the increase in the number of points per wavelength as frequency decreases which, as discussed in Section III.A, causes a small increase in the estimated stress. The error can also be seen to increase near to each end of the beam. As outlined in Section II.A, the gradient function uses a single-sided difference calculation at the end points of the beam, resulting in lower accuracy compared to the rest of the points considered. The beam also has a free boundary

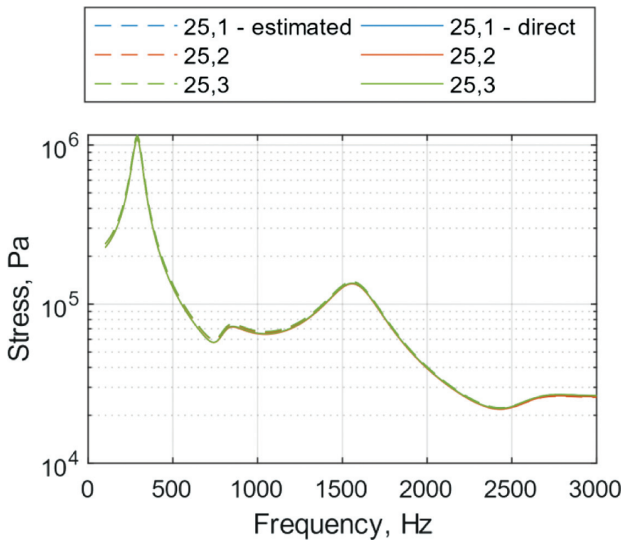

Fig. 5. Estimated and direct stress plotted against frequency for three points across the width of the beam, at points halfway along its length.

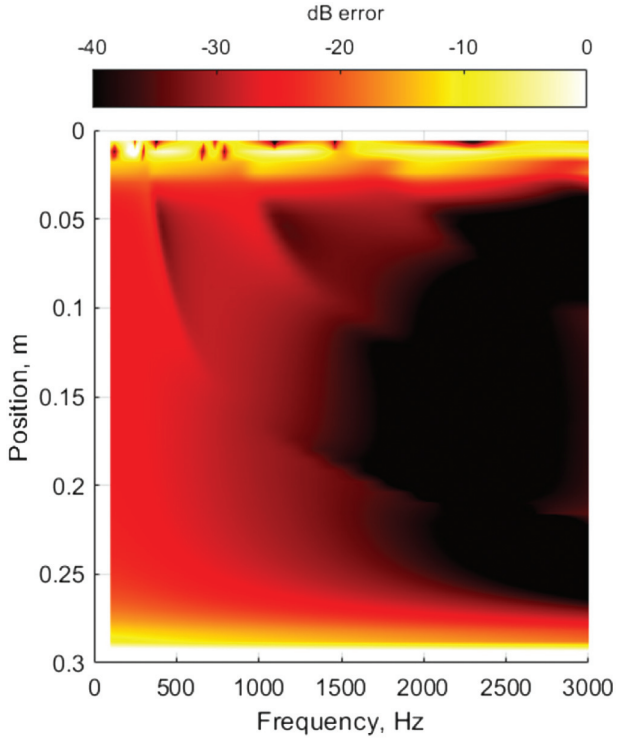

Fig. 6. Error in dB plotted against frequency for all positions at which the estimation is carried out along the length of the beam.

condition at each end, resulting in a zero stress condition, which increases the size of the relative error at these points. The high error at the $x = 0$ end of the beam is thought to be caused by proximity to the point force, applied 10mm from the end of the beam. Near to the point force it is unlikely that the stress is uniform across the width of the beam, so Euler–Bernoulli beam theory is no longer satisfied, resulting in larger errors in the estimation. To validate this, the estimated and direct stress at three points across the width of the beam at the x position closest to the point force are shown in Fig. 7. This shows that there is a significant difference in the stress across the width of the beam close to the point force and demonstrates the significant error in the stress estimation in this region. Inspection of Fig. 7 also explains the fluctuation in the error near to the point force over frequency, showing that at the central point the estimation becomes more accurate when the stress is high and less accurate when the stress is low.

In order to further investigate the behavior of the stress estimation method, the estimated stress is plotted against frequency and position along the middle of the three lines of points along the length of the beam in Fig. 8. The first four mode shapes of the structure can be observed in this plot as the red and yellow regions of high stress, showing how the stress peaks at the modal frequencies. By comparing the stress in Fig. 8 with the error in Fig. 6, it can be seen that the curved lines of low error correspond to the stress nodes of the response shapes. Figure 8 also shows a trend for stress to increase as frequency decreases, which could be causing small errors in the estimation due to violation of Euler–Bernoulli beam theory, since it is only valid for small beam deflections.

It has been shown that there are three main sources of error in the stress estimation method for the set of

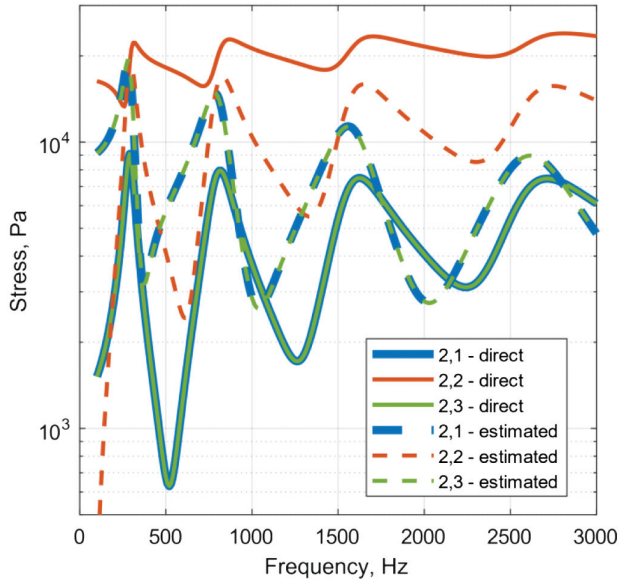

Fig. 7. Estimated and direct stress plotted against frequency for three points across the width of the beam at the x position closest to the point force.

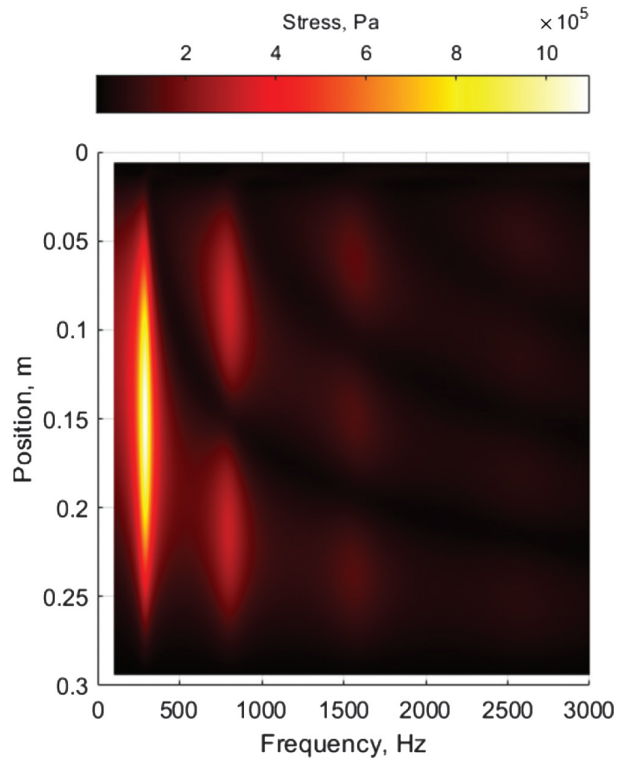

Fig. 8. Stress amplitude plotted against frequency for all positions along the length of the beam.

parameters considered in this section. The first occurs when the beam is not in pure bending, so the stress varies across the width of the beam. The second occurs when the level of stress in the beam is high, and the corresponding large deflections in the beam are not within the bounds of Euler–Bernoulli beam theory. The third is due to small numerical rounding errors that are amplified by the numerical derivative, the effect of which becomes more significant as the number of points per wavelength increases.

V. PARAMETRIC STUDY

It has been shown in the previous section that the accuracy of the stress estimation method is dependent on the number of points used in the estimation and variations of stress across the width of the beam. More specifically, it has been shown in Section IV that the accuracy of the stress estimation is dependent on the number points per wavelength. Since the wavelength depends on both the material and geometric properties of the structure, this section explores their effect on the stress estimation accuracy via a parametric study of Young's modulus, density, beam thickness, and isotropic loss factor.

The number of points used for the stress estimation in this study has been chosen based on the results presented in Section IV.A, where it was concluded that the number of points must be sufficient for there to be at least 10 points per wavelength at the highest frequency of interest. In this study, this must be the case for the entire range of parameters under consideration, so the number of points in the estimation has been chosen based on the set of parameters that result in the shortest wavelength within the considered frequency range. The parameter values in question are $E = 10^8$ and $\rho = 10^6$, in which case the thickness of the beam and the isotropic loss factor are as listed in Table I. Based on these parameters, 599 points along the length of the beam will be used for the stress estimation, resulting in a wavenumber of $\nu = 0.1$ occurring at approximately 3600 Hz.

Initially, a range of values for both Young's modulus, E, and density, ρ, have been considered, with E ranging from 10^8 to 10^{12} and ρ ranging from 10^2 to 10^6. The other beam parameters remain consistent with the values indicated in Table I. The mean percentage error across frequency has been calculated for each set of parameters for the stress estimation carried out at the center point of the beam in both the x and y directions. Figure 9 shows the resulting percentage error averaged across frequency for all the parameter values considered. Examination of these results shows that for low values of ρ and high values of E, the percentage error of the estimation is low; however, the error begins to increase as ρ increases and E decreases. This increase in error can be related to the decrease in the wavelength of vibration in the structure, as described by Equation (4), since above a given frequency the beam will no longer be bending only in the x direction. The blue dotted line shows the parameters for which the wavelength is equal to double the width of the beam at 3 kHz, since the first mode of bending across the width of the beam occurs when half a wavelength fits into the width of the beam. The green dotted line represents the parameters for which the wavelength is equal to the width of the beam at 3 kHz. Figure 9 shows that the increase in the error in the stress estimation begins somewhere between the two lines, suggesting that the error is caused by bending of the beam in the y direction, causing stress variations across the width. Based on this, it is likely that the accuracy of the stress estimation would be increased if a narrower beam was considered.

To provide further insight into the limitations of the stress estimation method, the estimation error has been calculated for a range of values of beam thickness, h,

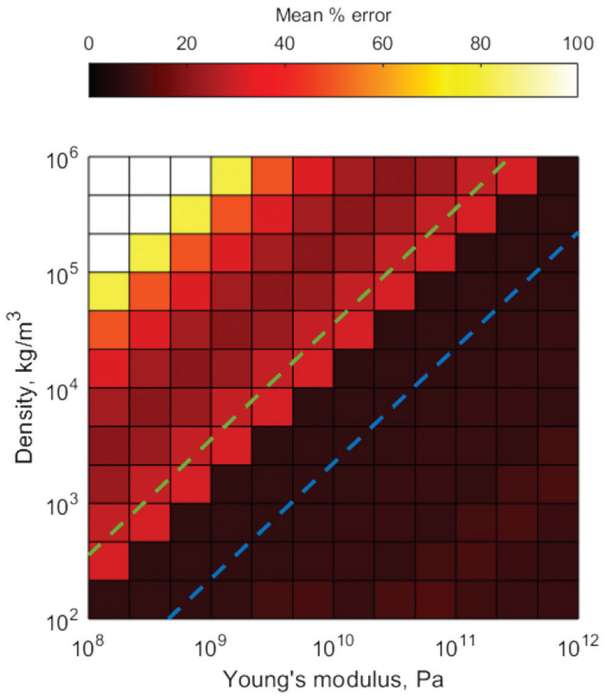

Fig. 9. Mean percentage error for a range of values of Young's modulus and density. The blue dotted line marks the parameter values where the beam width is equal to half a wavelength at 3 kHz and the green dotted line marks the parameter values where the width of the beam is equal to a full wavelength at 3 kHz.

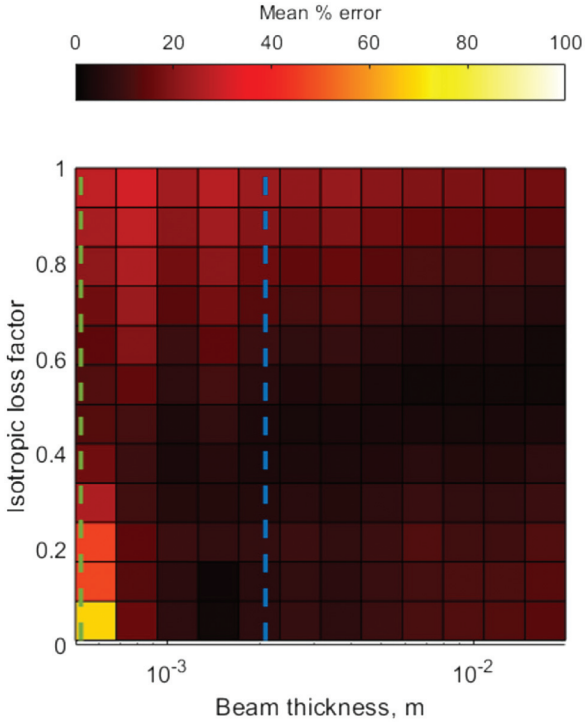

Fig. 10. Mean percentage error for a range of values of beam thickness and isotropic loss factor. The blue dotted line marks the parameter values where the beam width is equal to half a wavelength at 3 kHz and the green dotted line marks the parameter values where the width of the beam is equal to a full wavelength at 3 kHz.

and isotropic loss factor, η, with h ranging from 0.5 to 20mm and η ranging from 0.01 to 1. As above, the other beam parameters remain consistent with the values indicated in Table I. The stress estimation is again carried out at the center point of the beam in both the x and y directions. While the isotropic loss factor does not impact the wavelength of vibration, the thickness of the beam does, with a thinner beam resulting in a longer wavelength. Figure 10 shows the percentage error averaged across frequency for all parameterizations of the beam thickness and loss factor. The material properties for which the wavelength of vibration is equal to twice the width of the beam at 3 kHz are represented by the blue dotted line, and those for which the wavelength is equal to the width of the beam at 3 kHz are shown by the green dotted line. The positioning of these lines on Fig. 10 suggests that bending waves across the width of the beam are only likely to contribute to high errors for the very thinnest beams considered here. In particular, it can be seen that the very thinnest and lightly damped case has very high error, but this is not the case for beams with the same thickness and higher damping. It is thought that in this case, the high error is caused by a combination of stress variations across the width of the beam and large deflections caused by low damping, which, in Section IV.B, have been shown to be two significant sources of error in the stress estimation. Examination of the points to the right of the green dotted line shows that the accuracy of the estimation is low for both thin and highly damped beams. It is thought that the error observed for thin beams is due to large deflections in the structure which violate Euler–Bernoulli beam theory and have been shown in Section IV.B to cause significant errors. The high error seen when damping in the structure is high is likely caused by the fact that Euler–Bernoulli beam theory does not account for damping in the structure. Another region of Fig. 10 with noticeably larger error is that where the beam thickness is large and the isotropic loss factor is small. In this case, the combination of relatively large deflections caused by low damping and the thickness of the beam likely result in a significant amount of shear stress in the structure. Since Euler–Bernoulli beam theory assumes pure bending, this results in significant errors in the estimation.

It has been shown by the results presented in this section that the most significant errors in the stress estimation occur when the beam is bending in the y direction as well as the x direction, since this causes stress variations across the width of the beam. The error in the estimation has also been shown to increase when the damping in the structure is very high or the beam is very thin, as well as for thick, lightly damped beams where shear stress becomes significant.

VI. APPLICATION TO DIFFERENT MATERIALS

The parametric study presented in the previous section demonstrates the limits of the presented stress estimation method when the parameters used to define the material in the numerical model are chosen over a range of values. Some of these material property combinations correspond to realistic materials, but many do not. Therefore, this section presents an assessment of the stress estimation method when the material parameters are chosen based

on a selection of materials commonly used in practical applications.

The materials chosen for this study are aluminum alloy, stainless steel, acrylic, and nylon, and their material parameters are listed in Table III. The numerical model has been run and the stress estimation carried out for each set of parameters, with a grid of points that meets the requirements outlined in Section IV The results of this study are shown in Fig. 11 which presents the direct and estimated stress against frequency for each case. The results for aluminum alloy and stainless steel show a very low error in the estimated stress, which is consistent with the results from the parametric study in the previous section since both materials have a high Young's modulus and relatively low density, such that the wavelength of vibration is considerably longer than the width of the beam for the frequency range of interest. The error in the stress estimation is much higher for both acrylic and nylon, with both showing significant deviation from the direct stress as frequency increases. This error in the stress estimation is not due to the number of points per wavelength, since both materials have a wavenumber of $\nu < 0.1$ within the frequency range of interest; however, both structures result in bending across the width occurring within the frequency range of interest, which is consistent with the error increasing with frequency.

Table III. Parameters used to define the materials considered in this study

Material	E, GPa	ρ, kg/m^3	η
Aluminum	70	2728	0.02
Stainless steel	190	7500	0.02
Acrylic	3.2	1190	0.2
Nylon	2.0	1150	0.5

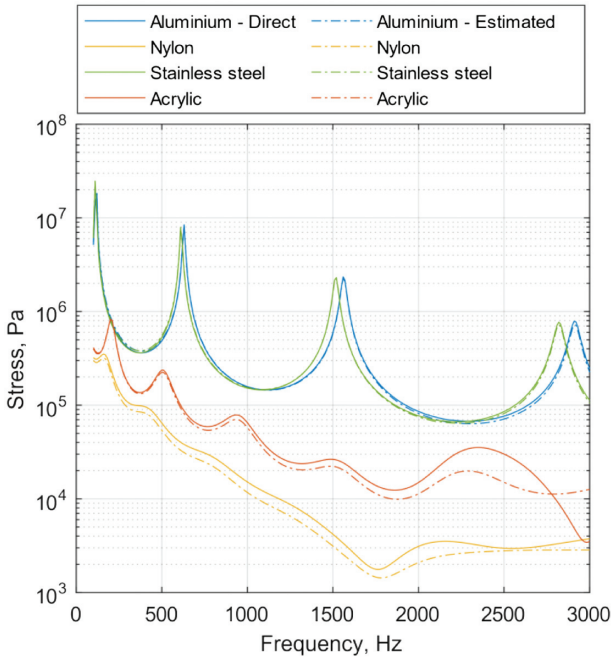

Fig. 11. Estimated stress and stress directly evaluated from the numerical model compared for a range of materials.

The results from this section provide more detail into the accuracy of the stress estimation method for beams manufactured from specific practical materials than provided by the averaged errors presented in the parametric study. The results, however, are consistent with the parametric study, showing that higher levels of error occur in heavily damped structures and that the error increases at frequencies where bending across the width of the beam is significant.

VII. CONCLUSIONS

This paper has presented a method for the estimation of stress in a uniform beam using Euler–Bernoulli beam theory, where deflection data evaluated at a grid of points across the surface of the beam is used to calculate the dynamic stress in the structure. The limitations of this method have been explored using a 2D numerical model of a uniform beam.

A validation of the estimation method has been carried out using a number of assessments, the first of which has shown that the number of points used for the estimation has a significant impact on its accuracy. The second assessment has shown that the position at which stress is estimated across the width of the beam does not significantly impact the accuracy of the method, provided that bending does not occur across the width of the beam, and that the position along the length is only significant at the points very close to the free ends of the beam, or near to a highly localized stress concentration. It has also been shown that small errors in the estimation method occur when the level of stress in the structure and the number of points per wavelength are high.

A parametric study has been carried out that explores the limits of the stress estimation method when applied to a beam with a range of material and geometric parameters. The study of Young's modulus and density has shown that the error in the stress estimation is high when the wavelength of vibration is short enough to cause bending across the width of the structure. The study of beam thickness and isotropic loss factor has shown that the stress estimation is less accurate when considering highly damped or thin structures, and that a thick, lightly damped structure will also result in a noticeable increase in error. The most significant errors in both parametric sweeps occur when bending across the width of the beam becomes significant, which is the case for thin beams, and those with low Young's modulus or high density.

The application of the stress estimation method to beams manufactured from commonly utilized commonly used for practical applications has shown that the stress in stiff, lightly damped structures is accurately predicted, whereas more flexible, highly damped structures tend to result in an increase in the estimation error.

This work has considered four parameters that affect the stress in a beam; however, there are other factors that could also impact stress and therefore affect the accuracy of the estimation. The width of the beam is known to have a significant impact on the accuracy of the estimate, since for a wider beam bending across the width will begin at a lower frequency. Another factor that could impact the accuracy of the estimation is if nonuniform beams were to be considered. Many practical structures have parameters that vary along the length of the structure, and this could result in a decrease in the accuracy of the estimation method. This study also assumes an ideal beam; however, in practice, a manufactured beam may have features such a surface roughness,

notches, and internal inhomogeneities that could result in stress concentrations in the structure that are not considered here. Future work could experimentally explore the effects of these factors on the accuracy of the stress estimation.

CONFLICT OF INTEREST STATEMENT

The authors declare no conflicts of interest.

REFERENCES

[1] F. V. Hunt, "Stress and strain limits on the attainable velocity in mechanical vibration," *J. Acoust. Soc. Am.*, vol. 32, pp. 1123–1128, 1960.

[2] E. E. Ungar, "Maximum stresses in beams and plates vibrating at resonance," *J. Eng. Ind.*, vol. 84, pp. 149–155, 1962.

[3] J. C. Wachel and J. D. Tison, "Vibrations in reciprocating machinary and piping systems," *EDI Rep.*, no. 335, pp. 85–305, 1985.

[4] F. J. Fahy, "Acoustic excitation of containing structures," PhD thesis, 1969.

[5] F. J. Fahy, "Statistics of acoustically induced vibrations," in *Proceedings of the Seventh International Congress on Acoustics*, Budapest, pp. 561–564, 1971.

[6] S. M. Stearn, "Stress distribution in randomly excited structures," Ph. D Thesis, Southampton University, 1970.

[7] S. M. Stearn, "Spatial variation of stress, strain and acceleration in structures subject to broad frequency band excitation," *J. Sound Vib.*, vol. 12, no. 1, pp. 85–97, 1970.

[8] F. J. Fahy and M. P. Norton, "Experiments on the correlation of dynamic stress and strain with pipe wall vibrations for statistical energy analysis applications," *Noise Control Eng. J.*, vol. 30, no. 3, pp. 107–117, 1988.

[9] M. P. Norton and D. G. Karczub, "Correlations between dynamic stress and velocity in randomly excited beams," *J. Sound Vib.*, vol. 226, no. 4, pp. 645, 674, 1999.

[10] M. P. Norton and D. G. Karczub, "Correlations between dynamic strain and velocity in randomly excited plates and cylindrical shells with clamped boundaries," *J. Sound Vib.*, vol. 230, no. 5, pp. 1069–1101, 2000.

[11] D. G. Karczub, "The prediction of dynamic stress and strain in randomly excited vibrating structures using vibrational velocity measurements," Ph. D Thesis. University of Western Australia, 1996.

[12] W. Hong, Z. Qin, K. Lv, and X. Fang, "An indirect method for monitoring dynamic deflection of beam-like structures based on strain responses," *Appl. Sci.*, vol. 8, no. 811, pp. 811–826, 2018.

[13] K. Y. Park, S. B. Jeon, Y. C. Park, and H. S. Lee, "Reconstruction of displacement, velocity and acceleration from measured dynamic strain for Bernoulli-beam type girders of bridges," *KSCE J. Civil Eng.*, vol. 27, no. 5, pp. 2104–2115, 2023.

[14] J. Tamayo, V. Pini, P. Kosaka, N. F. Martinez, O. Ahumada, and M. Calleja, "Imaging the surface stress and vibration modes of a microcantelever by laser beam deflection microscopy," *Nanotechnology*, vol. 23 Article ID 315501, 2012.

[15] R. N. Miles, W. Bao, and Y. Xu, "Estimation of random bending strain in a beam from discrete vibration measurements," *J. Sound Vib.*, vol. 174, pp. 191–199, 1995.

[16] R. N. Miles and Y. Xu, "Full-field random bending strain measurement of a plate from vibrational measurements," *J. Sound Vib.*, vol. 191, pp. 847–858, 1996.

[17] C. A. Moccio and R. N. Miles, "Measurement of the transfer function between bending strain and a transient load using a scanning laser vibrometer," *J. Sound Vib.*, vol. 189, pp. 611–699, 1996.

[18] R. G. Budynas and W. C. Young, *Roark's Formulas for Stress and Strain*, 7th ed.: McGraw-Hill, New York, 2002.

[19] R. M. Alford, K. R. Kelly, and D. M. Boore, "Accuracy of finite-difference modelling of the acoustic wave equation," *Geophysics*, vol. 39, pp. 834–842, 1974.